

FREQUENCY-DEPENDENT IMPEDANCE, MODULUS AND DIELECTRIC STUDIES OF POLYANILINE/MANGANESE DIOXIDE NANOCOMPOSITES

S. C. VELLA DURAI^{a,*}, E. KUMAR^b

^a*Department of Physics, JP College of Arts and Science, Agarakattu, Tenkasi, Tamilnadu, India*

^b*School of Science, Department of Physics, Tamil Nadu Open University, Chennai. Tamilnadu, India*

Structural properties, electric impedance, electric modulus and dielectric spectra properties have been used to investigate a Polyaniline/Manganese dioxide (PANI /MnO₂) nanocomposites prepared by in situ polymerization method. Prepared nanocomposites were analyzed by AC impedance spectroscopy. Pure PANI and MnO₂ nanoparticles have good crystalline nature, but when it was prepared to nanocomposites, crystalline nature could be change. When the concentration of MnO₂ nanoparticles has increased in nanocomposites, crystalline behaviour has been increases. Impedance studies were used to explain the electrode process. The modulus data of nanocomposites were analyzed as a function of different frequency range at a particular temperature. At low-frequency range, all the values of a real part of the electric modulus remain almost near to zero. Dielectric constant and dielectric loss have explained in brief. The impedance analysis was confirming the non-debye nature of the materials.

(Received March 25, 2020; Accepted June 12, 2020)

Keywords: Frequency, Dielectric, Modulus, Impedance, Nanocomposites, Temperature

1. Introduction

Nowadays, there has been a very high advantage in finding new solid-state devices with high conductivity for the application of batteries [1]. The mobile equipments and other electric equipments are growing out for energy storage devices [2]. As used for maintaining power, there are some defects in batteries and applications [3]. Therefore, metal oxides and conducting polymer have been found as the most promising materials for good application of energy storage devices [4]. The metal oxide has been regarded as easily prepared advantages. The conducting polymer is promising due to the fast doping mechanism, controllable conductivity, high environmental stability, high specific capacitance and very poor mechanical property applications [5]. In the last few years, considerable application carried out to the unique advantage of conducting polymer and metal oxide [6]. So, some material may not own all good characteristics, thus combining some different materials of needed characteristics find in far more efficient materials [7]. Some good and critical concentration of the metal oxide materials should be dispersed within the conducting polymer matrix to transfer the nanocomposite materials from the semiconducting state to a conducting state [8]. Polymer nanocomposites have good advantages of lightweight, low size, and low cost [9]. Polymer nanocomposites are more attractive materials for many applications with high advantages [10].

An impedance spectroscopy study gives fundamentals mechanisms of the basic electrical properties of the materials [11]. The impedance spectra studies are a tool of the electrical properties of all materials and give to details about the relaxation process of the prepared materials [12]. It explains the investigation of intrinsic material such as the frequency dependence of imaginary and real parts of impedance [13]. Some materials possessing good dielectric properties are wished for many applications in much energy stored devices such as transistors,

* Corresponding author: duraipee@gmail.com

sensors, and capacitors [14]. Electric properties materials contain good dielectric constant (ϵ') have been examining for many applications such as high charge-storage capacitors [15].

Some methods of preparation materials have been investigated to increase their dielectric constant although precede towards the addition of maximum dielectric constant ceramics to the elastomeric matrix [16]. Our knowledge from the litterateur survey, there is no report on comparative studies of polyaniline / manganese dioxide nanocomposites materials. Polymer composites with very low dielectric loss have many applications in the electronic field. Also, structural analysis, dielectric data such as dielectric loss, electric impedance, and electric modulus have been studied in polyaniline/ manganese dioxide nanocomposites. Accordingly, we were prepared different weight percentages (1, 5, and 10) polyaniline / manganese dioxide nanocomposites via in situ polymerization and investigated their impedance behaviour at various frequencies. Impedance, modulus, and dielectric response of the nanocomposites were studied in the frequency range of 10 μ Hz to 8 MHz at particular temperature of 50⁰C.

2. Experimental method

2.1. Materials

Aniline, ammonium persulphate, HCl, MgSO₄, MnC₂O₄, NaOH, and deionized water are used to prepare the nanoparticles and nanocomposites. The above-mentioned chemicals were purchased by MERCK (AR grade) and RANBAXY (AR grade).

2.2. Synthesis of PANI/ MnO₂ nanocomposite (One, Five and Ten Weight Percentage)

The MnO₂ nanoparticle using the materials like MnSO₄, MnC₂O₄, and NaOH was prepared by the microwave-assisted solution method. The PANI nanoparticles, using the materials like polyaniline, ammonium persulphate, and de-ionized water was prepared by in situ polymerization. Then three different beakers are used in this method, one beaker contains a mixture of 70 ml of HCl (2M) and 0.09g of MnO₂ nanoparticles, the second beaker contains a mixture of 70 ml of HCl and 0.45g of MnO₂ nanoparticles, the third beaker contains a mixture of 70 ml of HCl and 0.9g of MnO₂ nanoparticles. The aniline (4.5 ml) was injected in drop vice in each reaction solutions when those beakers are stirred at 40⁰C. The prepared three solutions after 6hour, The 4.5 g of ammonium persulphate were mixed in three different 20ml deionized water and solution was prepared. This solution is mixed drop by drop with a prepared solution which being stirred. The solution is stirred for three hours. It is kept at 100⁰C for two days in a vacuum with a view to obtain a green powder finally.

2.3. Experimental

Using X-ray diffractometer (XPRT-PRO using CuK α 1, λ =1.540 nm radiations), the prepared nanoparticles and nanocomposites are analyzed. The scattered angle of the above said analysis is 10⁰ to 80⁰ (2 θ values). AC impedance spectroscopic analysis was performed using a computer-controlled Zahnner zennium IM6 meter within the frequency range 10 μ Hz to 8 MHz at different temperatures.

3. Results and discussion

3.1. XRD Analysis

Fig. 1 shows XRD spectra of pure nanoparticles and nanocomposite materials. A broad peak at 25⁰ and a small peak at 14⁰ are characteristic peaks of PANI. Peaks for MnO₂ are present at 25⁰ (2 2 0), 28⁰ (3 1 0), 36⁰ (4 0 0), 39⁰(3 3 0), 42⁰(3 0 1), and 50⁰ (4 1 1) in accordance with JCPDS card no. 44-0141 [17]. However, in all the weight percentage nanocomposites, a very weak peak for MnO₂ at 28⁰ appeared shows that MnO₂ is fully injected and well dispersed in PANI Chain. With increasing weight percentage of PANI and MnO₂, intensity of the characteristic peak

of PANI at 25° is decreased suggesting and PANI are interacting with each other. Average crystalline size has been calculated using the Scherer formula given by

$$D = \frac{0.94\lambda}{\beta \cos\theta}$$

where λ is the wavelength, β the full width at half maximum, and θ the diffraction angle, the average crystalline size of PANI and MnO_2 nanoparticle is found as around near 9 [18] and 20 nm [17]. From the fig. 1 confirms that the PANI/ MnO_2 nanocomposite crystalline nature increasing with increases in the concentration of MnO_2 . So one and five weight percentage of nanocomposites have non-crystalline behaviour but ten weight percentages composite has good crystalline nature. Average crystalline size of the nanocomposites (10 wt%) diameter is 49 nm.

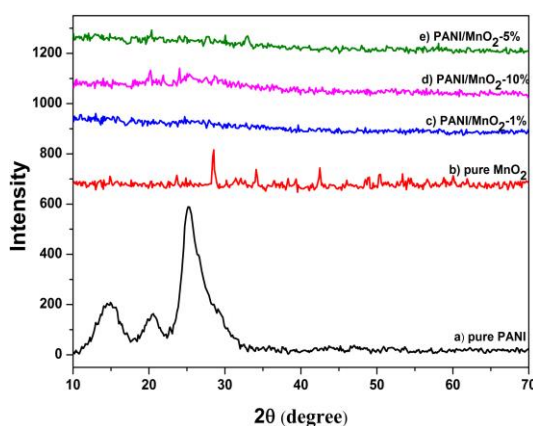


Fig. 1. XRD pattern of pure nanomaterials and nanocomposites materials.

3.2. Impedances analysis

The Cole-Cole plot is a well-known method. It is a wonderful tool which has been used for complete explains the electrical properties of the materials such as impedance of grain boundaries, and electrodes [19]. It gives the information about the real part (resistive) and imaginary part (reactive) of the material [20]. Cole-Cole plot typically comprises of one successive semicircle, it is due to the bulk properties at high-frequency region of the prepared pure and nanocomposite materials [21]. Cole - Cole plot shows representation of Z' versus Z'' [22]. Fig. 2 shows the cole - cole plots of the PANI/ MnO_2 nanocomposites as a function of MnO_2 concentration. Cole - Cole plots of the nanocomposites filled with 1, 5, and 10 weight percent of MnO_2 , as shown in fig. 2 display a semicircle shape indicating the presence of polarization with a single relaxation time. The centre of the semicircle explains the distance between nanoparticles. The radius of the semicircle gives the information about the nanocomposite resistance. The radius of the semicircle of the nanocomposites decreased with the increase in the weight percentage of MnO_2 content, decrease in nanocomposite resistivity. From the plot (nanocomposites materials), semi-circles are found and indicating a non-Debye type of relaxation process. According to the Maxwell–Wagner two-layer model, the phenomena are typically related to the existence of a distribution of relaxation time. The impedance of a system at an applied frequency can be written as some of the real and imaginary parts.

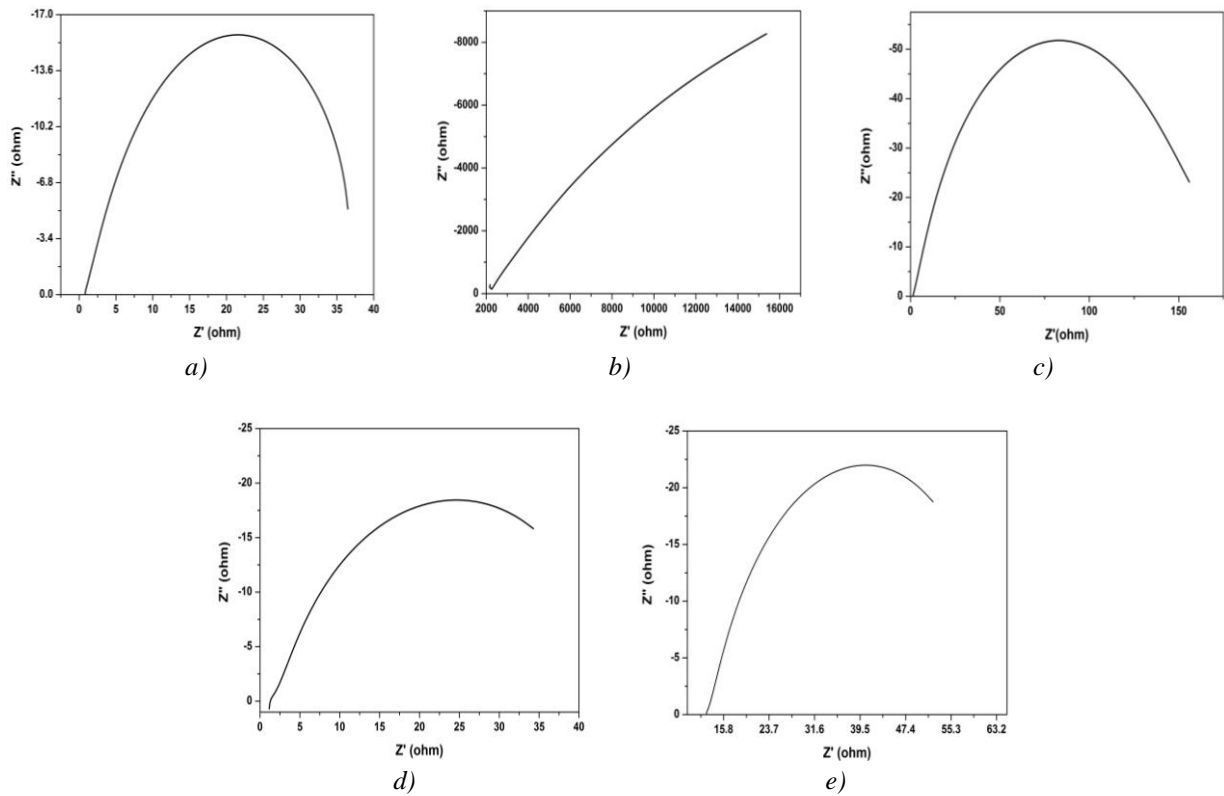


Fig. 2. Cole-Cole Plot of a) PANI, b) MnO_2 , c) 1wt%, d) 5wt% and e) 10wt%.

3.3. Modulus analysis

Fig. 3 & 4 demonstrate the plots of M' and M'' plotted against of angular frequency [23] for pure PANI, MnO_2 nanoparticles and all weight percentage (1, 5 & 10) nanocomposite materials. As angular frequency is increased, M' increases and reaches at a high value, i.e; PANI/ MnO_2 nanocomposite material is capacitive behaviour. It increases and reaches a high-value M'' shows relaxation phenomenon [24]. The imaginary part of modulus (M'') versus angular frequency spectra tell to relaxation mechanism, which measured at high frequencies, was contributed to interfacial polarization [25]. In Fig. 4 the peak shifts to higher frequency with the increasing of MnO_2 nanocomposite concentrations. Fig. 4 shows also that the height of the peak increase and constant with the MnO_2 nanocomposite concentration as relaxation time changes. Then it starts increasing with further increase in angular frequency. For pure nanoparticles, high value of M'' shifts to the low-frequency region as compare to other PANI/ MnO_2 nanocomposite materials with particular temperature. As charge carriers are able to move short distances at lower and higher frequencies, respectively.

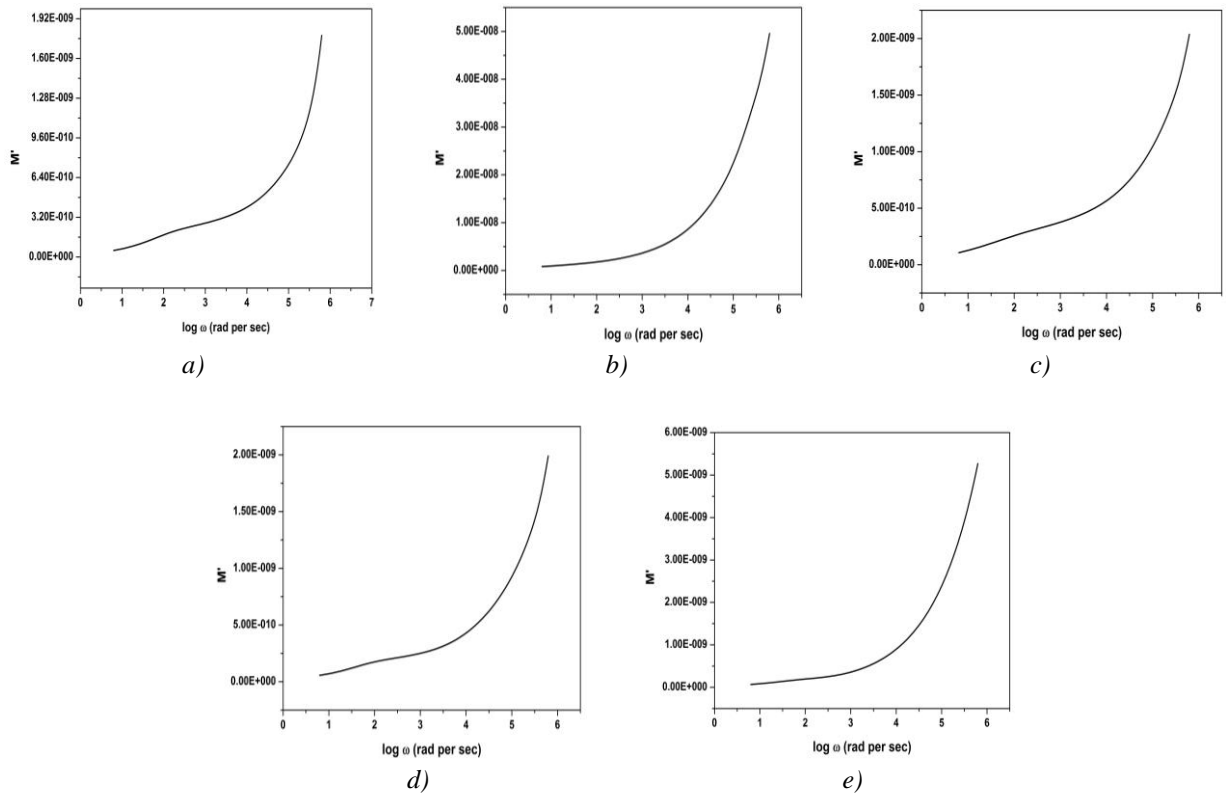


Fig. 3. Real modulus plot of a) PANI, b) MnO_2 , c) 1wt%, d) 5wt% and e) 10wt%.

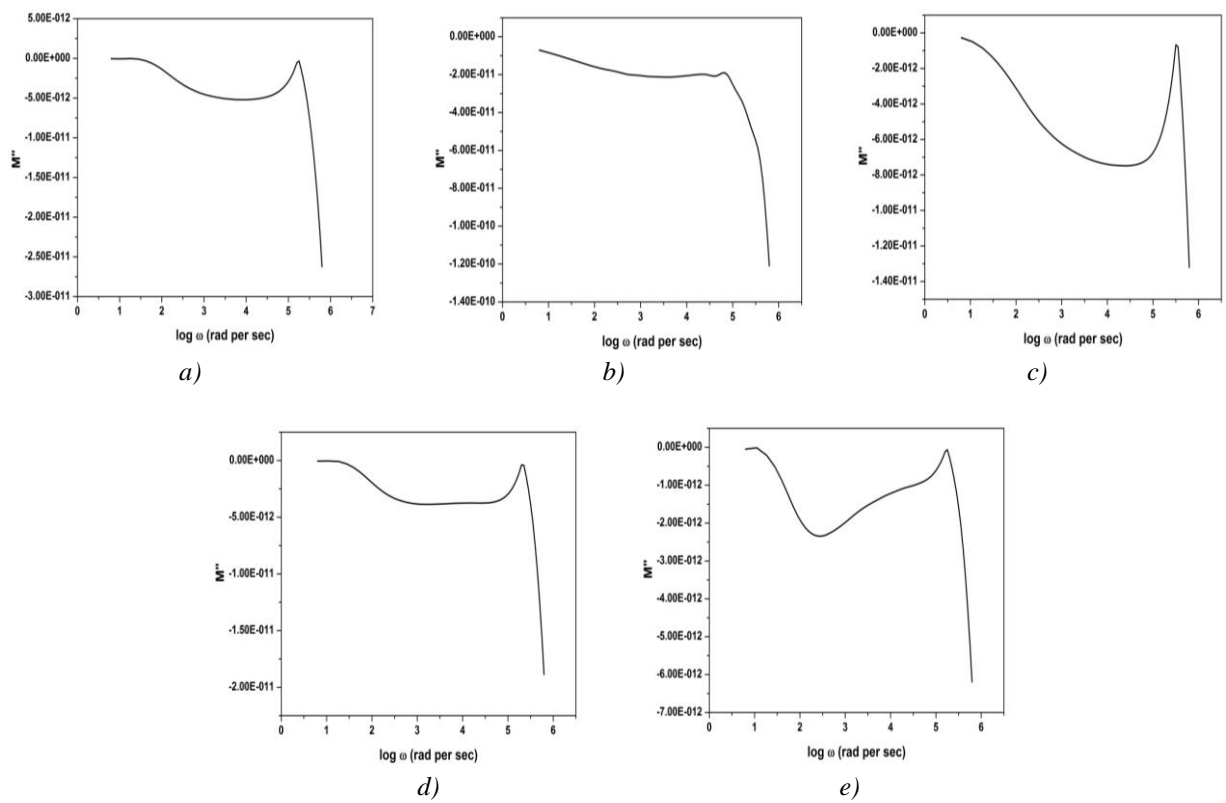


Fig. 4. Imaginary modulus plot of a) PANI, b) MnO_2 , c) 1wt%, d) 5wt% and e) 10wt%.

3.4. Dielectric analysis

Fig. 5 shows the variation of the real part of dielectric permittivity (ϵ') or dielectric constant with frequency for different weight percentage (1,5, & 10) at a particular temperature (50°C). All nanocomposites material, at low angular frequencies (ω) area dielectric constant, is starting to decrease. Dielectric constant is decreased with particular frequency increasing up to 2 to 2.5 rad per sec. But pure PANI nanoparticles at low-frequency region have near to zero, and then continues to decrease with increasing frequency. This is explaining in the low-frequency area, the conversion of the field is low. It is giving information about taken to sufficient time, to permanent and induced dipoles to align them dependent to the applying field, leading to inflate polarization. High values of dielectric constant confirm at low-frequency region area can be assign electrode polarization and interfacial polarization. Electrode polarization is associated with space charges at the electrodes and is studies by very high values of both imaginary and real part of permittivity [26]. Prepared all nanocomposites were analysis under good atmospheric conditions, having similar geometrical properties and composition. All prepared nanocomposites material, at high angular frequencies (ω) area dielectric constant, is start to increase up to zero [27]. But pure MnO_2 nanoparticles at high-frequency region have near to zero, and then continues to increase with increasing frequency.

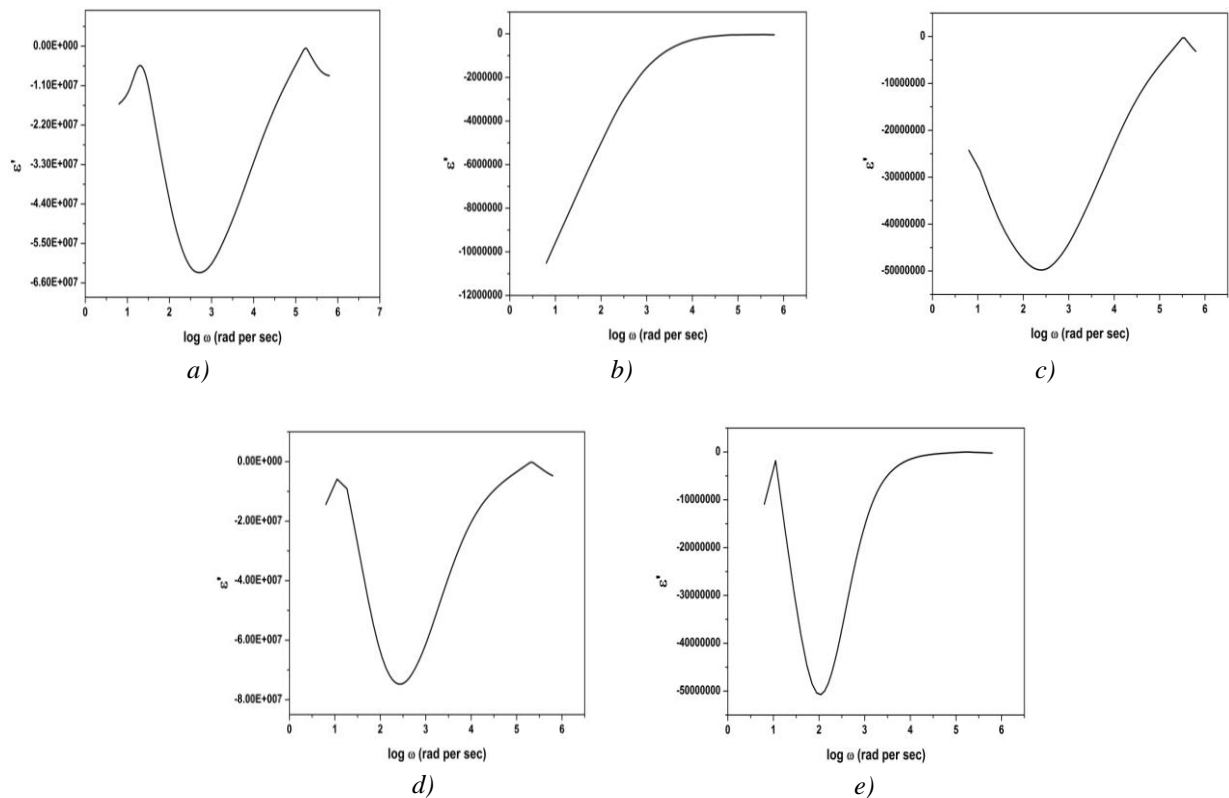


Fig. 5. Dielectric constant plot of a) PANI, b) MnO_2 , c) 1wt%, d) 5wt% and e) 10wt%.

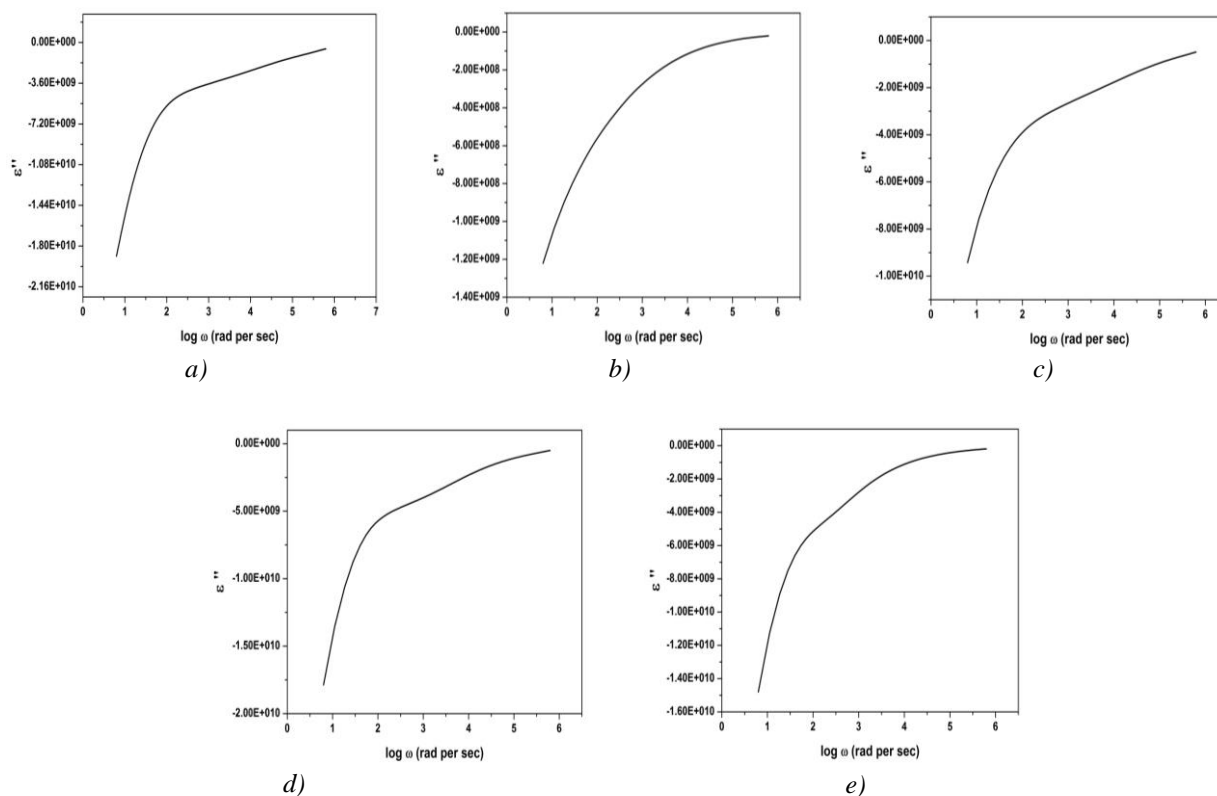


Fig. 6. Dielectric loss plot of a) PANI, b) MnO_2 , c) 1wt%, d) 5wt% and e) 10wt%.

Under this view, the higher values of (ϵ') is contributed to increase conductivity and interfacial polarization. Interfacial polarization explains the accumulation of limitless charges at the interface of the constituents, where they form very large dipoles. Its intensity is linked to the expanse of the occurring interfacial area within the nanocomposite system, giving thus indirect proof of the achieved distribution of nano inclusions. Fig. 5 was measured a systematic changes of (ϵ') in all nanocomposites samples. Since polarization and the stored energy is directly proportional to permittivity. Dielectric loss (ϵ'') was increased with increasing of nanocomposite weight percentage, and the peaks shift to increase with an increase of the frequency. Fig. 6 shows the variation of the dielectric loss (ϵ'') as a task of frequency and MnO_2 nanoparticles. ϵ'' is obtained for the conductance of the material, it increases with increasing frequency and increases with increasing MnO_2 nanoparticles concentration. In nanocomposite materials, plot of $\log \epsilon''$ versus $\log \omega$ can be found to distinguish between the offering of different conduction processes on ϵ'' [28].

4. Conclusion

PANI/ MnO_2 nanocomposites were synthesized in three different weight percentages. The structural, impedance, modulus and dielectric properties of the nanocomposites are analysis by powder x-ray diffraction (XRD), and AC impedance spectroscopy in a frequency range of frequencies from 10 μ Hz to 8 MHz. The impedance behaviour has been observed from a cole-cole plot. The polarization effect and distribution of ions has been observed from modulus analysis. The Maximum dielectric constant was observed in the high-frequency region, the relaxation process also observed from the dielectric analysis.

References

- [1] J. Schnell, F. Tietz, C. Singer, A. Hofer, N. Billot, G. Reinhart, *Energy Environ. Sci.* **12**(6), 1818 (2019).
- [2] L. Yao, B. Yang, H. Cui, J. Zhuang, J. Ye, J. Xue, *J. Mod. Power Syst. Clean Energy* **4**(4), 519 (2016).
- [3] Y. He, B. Matthews, J. Wang, L. Song, X. Wang, G. Wu, *J. Mater. Chem. A.* **6**(3), 735 (2018).
- [4] L. Fu, Q. Qu, R. Holze, V. V. Kondratiev, Y. Wu, *J. Mater. Chem. A.* **7**(25), 14937 (2019).
- [5] Z. Ma, W. Shi, K. Yan, L. Pan and G. Yu, *Chem. Sci.* **10**(25), 6232 (2019).
- [6] A. K. Mishra, *Journal of Atomic, Molecular, Condensate and Nano Physics.* **5**(2), 159 (2018).
- [7] J. M. Allwood, M. F. Ashby, T. G. Gutowski, E. Worrell, *Philos Trans A Math Phys Eng Sci.* **2013**, 20120496 (1986).
- [8] S. Vyas, S. Shivhare, A. Shivhare, *International Journal of Research and Scientific Innovation* **4**(7), 86 (2017).
- [9] P. H. C. Camargo, K. G. Satyanarayana, F. Wypych, *Mat. Res.* **12**(1), 1 (2009).
- [10] D. R. Paul, L. M. Robeson, *Polymer* **49**(15), 3187 (2008).
- [11] Y. Ben Taher, N. Moutia, A. Oueslati, M. Gargouri, *RSC Adv.* **6**(46), 39750 (2016).
- [12] K. R. Nandan, A. Ruban Kumar, *Journal of Materials Research and Technology* **8**(3), 2996 (2019).
- [13] Z. V. Mocanu, G. Apachitei, L. Padurariu, F. Tudorache, L. P. Curecheriu, L. Mitoseriu, *European Physical Journal: Applied Physics, EDP Sciences* **56**(1), 10102 (2011).
- [14] Zhicheng Shi, Jing Wang, Fan Mao, Chaoqiang Yang, Chao Zhang, Runhua Fan, *J. Mater. Chem. A* **5**(28), 14573 (2017).
- [15] M. Guo, T. Hayakawa, M. Kakimoto, T. Goodson, *The journal of physical chemistry. B* **115**(46), 13419 (2011).
- [16] Liyun Yu, Frederikke Bahrt Madsen, Søren Hvilsted, Anne Ladegaard Skov, *RSC Adv.* **5**, 49739 (2015).
- [17] E. Kumar, S. C. Vella durai, L. Guru Prasad, D. Muthuraj, V. Bena Jothy, *Journal of Materials and Environmental Sciences.* **8**(10), 3490 (2017).
- [18] A. Mostafaei, A. Zolriasatein, *Progress in Natural Science: Materials International* **22**(4), 273 (2012).
- [19] Tanusree Mondal, Sayantani Das, T. P. Sinha, P. M. Sarun, *Materials Science-Poland* **36**(1), 112 (2018).
- [20] A. Bagum, M. B. Hossen, F. U. Z. Chowdhury, *Ferroelectrics* **494**(1), 19 (2016).
- [21] R. N. P. Choudhary, S. Dutta, A. K. Thakur, P. K. Sinha, *Ferroelectrics* **306**(1), 55 (2004).
- [22] Z. Imran, a M. A. Rafiq, M. Ahmad, K. Rasool, S. S. Batool, M. M. Hasan, *AIP Advances* **3**(3), 032146 (2013).
- [23] M. Belal Hossen, A. K. M. Akther Hossain, *Journal of Advanced Ceramics* **4**, 217 (2015).
- [24] R. V. Barde, K. R. Nemade, S. A. Waghuley, *Journal of Asian Ceramic Societies* **3**(1), 116 (2015).
- [25] T. F. Khoon, J. Hassan, Z. A. Wahab, R. S. Azis, *Engineering Science and Technology, An International Journal* **19**(4), 2081 (2016).
- [26] C. Chassagne, E. Dubois, M. L. Jiménez, J. P. M. van der Ploeg, J. V. Turnhout, *Front Chem.* **4**, 30 (2016).
- [27] S. Mahmood, S. Nasir, G. Asghar, M. Iftikhar, R. Hussain, G. Xing, *Journal of Ovonic Research* **15**(2), 95 (2019).
- [28] G. Mustafa, M. Ul Islam, *Journal of Ovonic Research* **15**(4), 227 (2019).